2,2,4,4,6,6-Hexabenzylcyclotristannatellurane, $(Bn_2SnTe)_3$. Synthesis and Structural Characterization of an Organometallic Single-Source Precursor to Phase-Pure, Polycrystalline SnTe

Philip Boudjouk,* Michael P. Remington, Jr., Dean G. Grier, Wayne Triebold, and Bryan R. Jarabek

Center for Main Group Chemistry, Department of Chemistry, North Dakota State University, Fargo, North Dakota 58105

Received July 1, 1999

The title compound, $(Bn_2SnTe)_3$, Bn = $CH_2C_6H_5$, was prepared in high yield by treating Bn_2SnCl_2 with $(NH_4)_2Te$. Details of the synthesis and characterization (^1H, ^{13}C, ^{119}Sn, and ^{125}Te NMR; IR, single-crystal XRD, and elemental analyses) are presented. $(Bn_2SnTe)_3$ serves as an efficient single-source precursor to phase-pure cubic SnTe under mild conditions

Introduction

Tin telluride and other tin chalcogenides are widely used as semiconductors.[1] For example, SnTe, with a direct E_g of 0.18 eV,[2] has found application in infrared detection, radiation receiving, and thermoelectric devices.[3] Interest in the structure and bonding of 14-16 materials has also driven research in this area.[4] Synthetic routes to these materials include heating mixtures of the elements at high temperatures for extended time periods,[5] reaction of the elements in liquid ammonia,[6] precipitation from aqueous solutions,[7] organometallic chemical vapor deposition (OMCVD),[8] solid-state metathesis,[9] and, more recently, pyrolysis of organometallic single-source precursors.[10]

We have demonstrated that ring systems of the type $(Bn_2SnE)_3$, (Bn = $CH_2C_6H_5$, E = S or Se) provide the 14-16 material in high yields and high purity by homolytic bond cleavage of the C−Sn bond.[10a] This route has the advantages of utilizing mild decomposition temperatures, producing an inert and easily removed organic byproduct, 1,2-diphenylethane, and controlling the stoichiometry of the end members as well as the corresponding solid solutions, SnS_xSe_{1-x}. Easy access to solid solutions allows tailoring of the band gap.[11]

Furthering our investigation of molecular precursors to 14-16 materials, we report here the synthesis, characterization, and decomposition of the novel six-membered ring containing alternating Sn and Te atoms, $(Bn_2SnTe)_3$. This compound serves as an organometallic single-source precursor to cubic SnTe under mild thermal conditions (≥200 °C). Homolytic bond cleavage of the Sn−C bond and the formation of 1,2-diphenylethane is the dominant mechanism.

Results and Discussion

Precursor Synthesis. Cyclic tin chalcogenides can be prepared by the reaction of a dialkyldihalostannane, R_2SnX_2, with alkali metal chalcogenolates, MEH,[12] or by treating elemental chalcogens with dialkylstannanes.[13] Recently we reported that these compounds are accessible in good to excellent yields from R_2SnX_2 and freshly prepared anhydrous alkali metal chalcogenides, M_2E[10a,c] (eq 1).

$$R_2SnX_2 + Na_2E \rightarrow 1/3(R_2SnE)_3 + 2\ NaX \quad (1)$$
$$R = Ph, Bn;\ E = S, Se$$

Attempts to produce the tellurium analogue, with R = Bn, in our laboratory by eq 1 failed. Typically, tellurium powder was the major product. However, when we use ammonium telluride, prepared as in eq

(1) Berger, L. I. *Semiconductor Materials*; CRC Press: New York, 1997.
(2) (a) Fouad, S. S.; Morsy, A. Y.; Soliman, H. S.; Ganainy, G. A. *J. Mater. Sci. Lett.* **1994**, *13*, 82. (b) Rogers, L. M. *Br. J. Appl. Phys.* **1968**, *1*, 845. (c) Esaki, L.; Stiles, P. J. *Phys. Rev. Lett.* **1966**, *16*, 1108.
(3) (a) George, J.; Palson, T. I. *Thin Solid Films* **1985**, 127, 233, and references therein. (b) Santhanam, S.; Chaudhuri, A. K. *Phys. Status Solidi A* **1984**, *83*, k77. (c) Reynolds, R. A. *J. Electrochem. Soc.* **1967**, *114*, 526. (d) Brebrick, R. F.; Strauss, A. J. *Phys. Rev.* **1963**, *131*, 104.
(4) (a) Lin, J.-C.; Ngai, T. L.; Chang, Y. A. *Metall. Trans. A* **1986**, *17A*, 1241. (b) Rabe, K. M.; Joannopoulos, J. D. *Phys. Rev. B* **1985**, *32*, 2302. (c) Miller, A. J.; Saunders, G. A.; Yogurtçu, Y. K. *J. Phys. C: Solid State Phys.* **1981**, *14*, 1569. (d) Littlewood, P. B. *J. Phys. C: Solid State Phys.* **1980**, *13*, 4855.
(5) (a) Greenwood, N. N., Earnshaw, A., Eds.; *Chemistry of the Elements*; Permagon: New York, 1990. (b) Blitz, W.; Mecklenburg, W. *Z. Anorg. Allg. Chem.* **1909**, 64, 226. (c) Abrikosov, N. K.; Bankina, V. F.; Poretskaya, L. V.; Shelimova, L. E. *Semiconducting II−VI, IV−VI, and V−VI Compounds*; Plenum: New York, 1969. (d) Yellin, N.; Ben-Dor, L. *Mater. Res. Bull.* **1983**, *18*, 823.
(6) Henshaw, G.; Parkin, I. P.; Shaw, G. A. *J. Chem. Soc., Dalton Trans.* **1997**, 231.
(7) Gorer, S.; Albu-Yaron, A.; Hodes, G. *Chem. Mater.* **1995**, *7*, 1243.
(8) Manasevit, H. M.; Simpson, W. I. *J. Electrochem. Soc.* **1975**, *122*, 444.
(9) Parkin, I. P.; Rowley, A. T. *Polyhedron* **1993**, *12*, 2961.
(10) (a) Boudjouk, P.; Seidler, D. J.; Grier, D.; McCarthy, G. J. *Chem. Mater.* **1996**, *8*, 1189. (b) Boudjouk, P.; Seidler, D. J.; Bahr, S. R.; McCarthy, G. J. *Chem. Mater.* **1994**, *6*, 2108. (c) Boudjouk, P.; Bahr, S. R.; McCarthy, G. J. *Chem. Mater.* **1992**, *4*, 383. (d) Seligson, A. L.; Arnold, J. *J. Am. Chem. Soc.* **1993**, *115*, 8214. (e) Cowley, A. H.; Jones, R. A. *Angew. Chem., Int. Ed. Engl.* **1989**, *28*, 1208.
(11) Pierson, H. O. *Handbook of Chemical Vapor Deposition (CVD): Principles, Technology and Applications*; Noyes Publications: Park Ridge, NJ, 1992.
(12) Blecher, A.; Dräger, M. *Angew. Chem., Int. Ed. Engl.* **1979**, *18*, 677.
(13) Blecher, A.; Mathiasch, B. *Z. Naturforsch. B* **1978**, *33*, 246.

10.1021/om990506u CCC: $18.00
Publication on Web 09/30/1999

Table 1. Crystallographic Data for $(Bn_2SnTe)_3$

empirical formula	$C_{42}H_{42}Sn_3Te_3$
fw	1285.63
temperature	298(2) K
wavelength	0.71073 Å
crystal system	triclinic
space group	$P\bar{1}$
unit cell dimens	$a = 11.2391(6)$ Å, $\alpha = 89.9940(10)°$ $b = 17.2765(8)$ Å, $\beta = 89.9750(10)°$ $c = 23.6362(12)$ Å, $\gamma = 75.4250(10)°$
volume	4441.8(4) Å^3
Z	4
density (calcd)	1.922 Mg/m^3
abs coeff	3.631 mm^{-1}
$F(000)$	2400
crystal size	0.35 × 0.45 × 0.65 mm^3
θ range for data collection	0.86−19.00°
index ranges	$-10 \le h \le 14$, $-21 \le k \le 23$, $-29 \le l \le 30$
reflns collected	12060
indep reflns	6950 [R(int) = 0.1616]
abs corr	none
refinement method	full-matrix least-squares on F^2
no. of data/restraints/params	6918/0/865
goodness-of-fit on F^2	1.075
final R indices [$I>2\sigma(I)$]	R1 = 0.0716, wR2 = 0.1814
R indices (all data)	R1 = 0.0762, wR2 = 0.1936
largest diff peak and hole	1.465 and −1.706 e Å^{-3}

2,[14] as the source of Te^{2-}, the reaction proceeds efficiently.

$$3Te + 6NH_4OH + 2Al \rightarrow 3(NH_4)_2Te + 2Al(OH)_3 \quad (2)$$

The reaction of a deoxygenated aqueous solution of ammonium telluride with an ether solution of dibenzyltin dichloride produces 2,2,4,4,6,6-hexabenzylcyclotristannatellurane, $(Bn_2SnTe)_3$, in very good yields (ca. 80%). A gray precipitate composed of SnTe, Te, and NH_4-Cl, as shown by X-ray powder diffraction (XRPD), is also produced.

Molecular Structure. Recrystallization of $(Bn_2SnTe)_3$ from Et_2O provides yellow crystals that are suitable for single-crystal X-ray diffraction (SCXRD). $(Bn_2SnTe)_3$ crystallizes in the triclinic space group $P\bar{1}$ with two independent molecules in the asymmetric unit.[15] Table 1 summarizes the crystal data and structure refinement. The molecular structure and atom-numbering scheme of $(Bn_2SnTe)_3$ are shown in Figure 1, selected bond distances and angles in Table 2, and atomic parameters in Table 3.

The $(SnTe)_3$ ring is in a distorted boat conformation. The geometry of the $(SnTe)_3$ ring is in excellent agreement with that of the methyl analogue, $(Me_2SnTe)_3$, with average Te−Sn−Te and Sn−Te−Sn bond angles of 113.41° and 95.82° vs 112.6° and 96°, respectively.[12] The tin atoms form a tetrahedron with an average C−Sn−C angle of 109.6° (ranging from 112.9° to 106.5°), distinctly more acute than the methyl analogue (av 113°).[12] The Sn−Te and Sn−C bond distances are similar to those reported for other Sn(IV)−Te ring structures.[12,16]

An interesting feature of the solid-state structure of $(Bn_2SnTe)_3$ is the packing of the molecules into infinite chains lying parallel to the b-axis. These chains superimpose along the a-axis. The shortest intermolecular nonbonding distances occur between the methylene proton of one benzyl group on each of Sn(2) and Sn(6) with the lone pair of electrons on neighboring tellurium atoms Te(4) and Te(3), respectively. These distances are 3.160 Å for H22a−Te4 and 3.192 Å for H78a−Te3 (Figure 1).

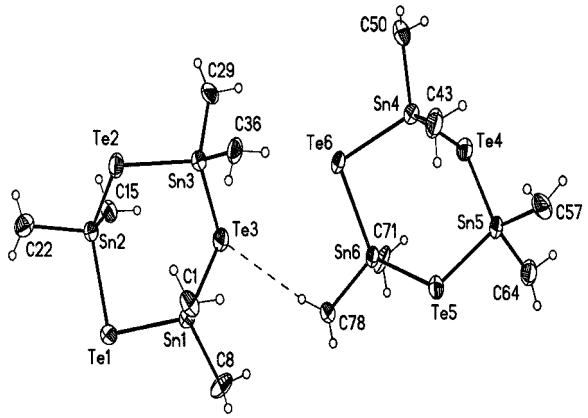

Figure 1. Molecular structure and atom-numbering scheme for the asymmetric unit of $(Bn_2SnTe)_3$. The phenyl groups of the benzyl moieties have been removed for clarity.

Table 2. Selected Bond Lengths [Å] and Angles [deg] for $(Bn_2SnTe)_3$

molecule 1		molecule 2	
Sn(1)−Te(1)	2.729(2)	Sn(4)−Te(6)	2.730(2)
Sn(1)−Te(3)	2.738(2)	Sn(4)−Te(4)	2.738(2)
Sn(2)−Te(2)	2.7368(15)	Sn(6)−Te(5)	2.7359(15)
Sn(2)−Te(1)	2.741(2)	Sn(6)−Te(6)	2.742(2)
Sn(3)−Te(3)	2.720(2)	Sn(5)−Te(4)	2.721(2)
Sn(3)−Te(2)	2.7322(15)	Sn(5)−Te(5)	2.736(2)
Sn(1)−C(1)	2.17(2)	Sn(4)−C(43)	2.17(2)
Sn(1)−C(8)	2.17(2)	Sn(4)−C(50)	2.16(2)
Sn(2)−C(15)	2.18(2)	Sn(5)−C(57)	2.18(2)
Sn(2)−C(22)	2.18(2)	Sn(5)−C(64)	2.21(2)
Sn(3)−C(29)	2.15(2)	Sn(6)−C(71)	2.15(2)
Sn(3)−C(36)	2.15(2)	Sn(6)−C(78)	2.15(2)
Te(1)−Sn(1)−Te(3)	111.24(5)	Te(6)−Sn(4)−Te(4)	111.32(5)
Te(2)−Sn(2)−Te(1)	115.71(5)	Te(5)−Sn(6)−Te(6)	115.68(5)
Te(3)−Sn(3)−Te(2)	113.28(5)	Te(4)−Sn(5)−Te(5)	113.20(5)
C(8)−Sn(1)−C(1)	112.9(10)	C(43)−Sn(4)−C(50)	111.1(8)
C(15)−Sn(2)−C(22)	109.5(6)	C(78)−Sn(6)−C(71)	109.6(8)
C(29)−Sn(3)−C(36)	106.5(7)	C(57)−Sn(5)−C(64)	108.0(7)
C(1)−Sn(1)−Te(1)	110.1(5)	C(43)−Sn(4)−Te(6)	109.1(5)
C(1)−Sn(1)−Te(3)	112.0(5)	C(43)−Sn(4)−Te(4)	112.3(5)
C(8)−Sn(1)−Te(1)	106.0(7)	C(50)−Sn(4)−Te(6)	106.6(5)
C(8)−Sn(1)−Te(3)	104.3(7)	C(50)−Sn(4)−Te(4)	106.2(6)
C(15)−Sn(2)−Te(1)	107.1(5)	C(71)−Sn(6)−Te(6)	107.0(5)
C(15)−Sn(2)−Te(2)	117.4(5)	C(71)−Sn(6)−Te(5)	118.1(5)
C(22)−Sn(2)−Te(1)	105.4(5)	C(78)−Sn(6)−Te(6)	105.5(4)
C(22)−Sn(2)−Te(2)	100.9(4)	C(78)−Sn(6)−Te(5)	99.9(5)
C(29)−Sn(3)−Te(2)	111.5(5)	C(57)−Sn(5)−Te(5)	104.1(4)
C(29)−Sn(3)−Te(3)	104.7(6)	C(57)−Sn(5)−Te(4)	116.5(5)
C(36)−Sn(3)−Te(2)	104.4(5)	C(64)−Sn(5)−Te(5)	110.9(5)
C(36)−Sn(3)−Te(3)	116.3(4)	C(64)−Sn(5)−Te(4)	104.1(5)
Sn(1)−Te(1)−Sn(2)	93.71(4)	Sn(4)−Te(6)−Sn(6)	93.66(4)
Sn(3)−Te(2)−Sn(2)	99.10(4)	Sn(5)−Te(5)−Sn(6)	99.13(5)
Sn(3)−Te(3)−Sn(1)	94.66(5)	Sn(5)−Te(4)−Sn(4)	94.65(5)

Synthesis and Characterization of SnTe. Pyrolysis of $(Bn_2SnTe)_3$ in a conventional flow pyrolysis unit at 200 or 275 °C, for 10 h, or at 400 °C for 5 h produced SnTe in high yield (eq 3). These low temperatures are comparable to those used in the preparation of SnTe from homoleptic Sn(II) tellurolates (ca. 250 °C).[10d]

(14) Nitsche, R. *Angew. Chem.* **1957**, *69*, 333.

(15) While the metric parameters suggest a monoclinic unit cell, the triclinic structure given here was the only setting that provided a satisfactory solution. The germanium analogue, $(Bn_2GeTe)_3$ (our unpublished results), however, which displays similar molecular geometry and intermolecular interactions, crystallizes in the monoclinic $P2_1/c$ space group.

(16) Puff, H.; Breuer, B.; Schuh, W.; Sievers, R.; Zimmer, R. *J. Organomet. Chem.* **1987**, *332*, 279.

Table 3. Selected Atomic Coordinates ($\times 10^4$) and Equivalent Isotropic Displacement Parameters ($Å^2 \times 10^3$) for $(Bn_2SnTe)_3$[a]

	x	*y*	*z*	*U*(eq)
Sn(1)	10441(1)	4588(1)	8033(1)	61(1)
Sn(2)	9556(1)	6078(1)	6722(1)	49(1)
Sn(3)	10478(1)	3611(1)	6491(1)	54(1)
Sn(4)	10439(1)	9589(1)	6967(1)	61(1)
Sn(5)	10480(1)	8609(1)	8509(1)	55(1)
Sn(6)	9558(1)	11079(1)	8279(1)	50(1)
Te(1)	9851(1)	6203(1)	7866(1)	63(1)
Te(2)	11299(1)	4913(1)	6189(1)	64(1)
Te(3)	8962(1)	3877(1)	7406(1)	65(1)
Te(4)	8962(1)	8877(1)	7594(1)	64(1)
Te(5)	11302(1)	9914(1)	8810(1)	64(1)
Te(6)	9851(1)	11204(1)	7133(1)	64(1)

[a] *U*(eq) is defined as one-third of the trace of the orthogonalized U_{ij} tensor.

$$(Bn_2SnTe)_3 \rightarrow 3SnTe + 3Bn_2 \qquad (3)$$

Thermolysis at the lower temperatures resulted in yields of SnTe slightly greater than predicted (av 102%), suggesting incomplete reaction and/or retention of organic species. Total mass recovery (nonvolatile + volatile products) was good at 85%. Trace combustion analysis of the ceramic product showed <1% carbon and hydrogen, which were reduced to <0.5% after rinsing of the ceramic product with solvent. These values are much lower than those observed for the SnTe prepared by homoleptic Sn(II) tellurolates (3.05% C, 0.74% H).[10d]

X-ray powder diffraction (XRPD) confirmed that the ceramic product was highly crystalline, phase-pure, cubic tin telluride with an average crystallite size > 1000 nm, as determined using the Scherrer equation (Figure 2). This is in contrast to the SnTe films produced by Ganainy et al. via a thermal evaporation technique, which contain a significant amorphous component in addition to crystalline SnTe.[2a]

Tin telluride crystallizes in the cubic [NaCl] (rock salt) structure, space group *Fm*3*m*. SnTe has a narrow homogeneity range of 0.9 atom % at 50% Te, toward the Te-rich side.[17] At compositions of $Sn_{1-x}Te_x$ with $x > 0.5$, the lattice parameter decreases relative to stoichiometric SnTe.[17] Unit cell parameters of the powders produced in this study lie within the range of previously reported values[10b,18a−e] and are shown in Table 4. The unit cell obtained in this study corresponds to approximately $Sn_{0.495}Te_{0.505}$ according to an equation produced by Brebrick relating unit cell length to stoichiometry for a series of tin tellurides.[18e] X-ray powder diffraction data for SnTe are given in Table 5.

When care is taken to avoid prolonged exposure of $(Bn_2SnTe)_3$ to light and air, no peaks attributable to crystalline tin, tellurium, or the oxides of these elements were observed in the pyrolysate. 1,2-Diphenylethane was the only volatile product detected, suggesting that the decomposition is dominated by homolytic Sn−C bond cleavage to form benzyl radicals followed by dimerization.[10a]

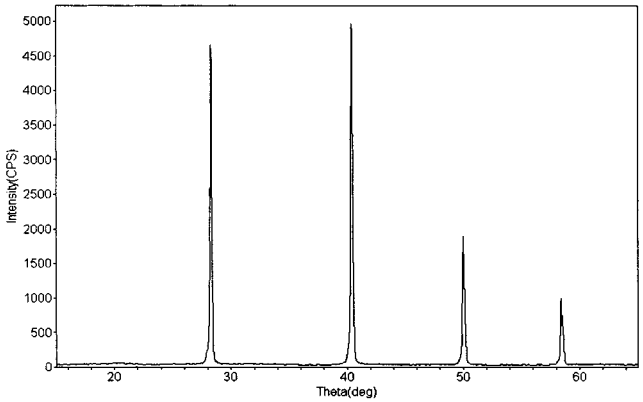

Figure 2. XRPD pattern of SnTe from pyrolysis of $(Bn_2SnTe)_3$ at 275 °C for 10 h.

Table 4. XRD Measured Unit-Cell Parameters for SnTe

reference	*a*, Å	volume, $Å^3$
PDF 8-487[18a]	6.303	250.4
PDF 25-465[18b]	6.3272	253.30
PDF 46-1210[18c]	6.32751(5)	253.337(6)
Bis and Dixon[18d]	6.312(2)	251.5
Brebrick[18e]	6.3017−6.3272	250.24−253.30
Boudjouk[10b]	6.3171(85)	252.098(9)
this study	6.30954(33)	251.18

Thermolysis at 400 °C for 5 h also produced highly crystalline, phase-pure, cubic tin telluride. Ceramic yields were 98% of theoretical, with the as-produced powders having a carbon and hydrogen content of <0.5%. The organic residue collected was 1,2-diphenylethane. Total mass recovery was 85%.

The electron micrograph of a typical sample produced at 275 °C shows individual SnTe grains, with typical sizes ranging from 0.3 to 0.5 μm in diameter, and morphologies of both cubes and mixtures of cubic and octahedral forms (Figure 3).

Conclusions

2,2,4,4,6,6-Hexabenzylcyclotristannatellurane was prepared in high yield by treating Bn_2SnCl_2 with aqueous $(NH_4)_2Te$. In the solid state, molecules of $(Bn_2SnTe)_3$ form infinite molecular chains lying parallel to the *b*-axis and superimposing along the *a*-axis.

Thermolysis of $(Bn_2SnTe)_3$ in an inert atmosphere under mild conditions produces polycrystalline, cubic SnTe in high yield and high purity. The SnTe crystals possess cubic and cubooctahedral morphologies and have a uniform size distribution of 0.3−0.5 μm in diameter.

Experimental Section

General Comments. Flow pyrolyses were performed using a Lindberg model 55035 programmable tube furnace, 36 cm long and 3 cm in diameter with a 55 × 2.5 cm Vycor silica glass tube placed inside. One end of the tube was fitted with a one-holed septum connected to a source of dry nitrogen and sealed with Parafilm. Nitrogen flow was monitored at the exit of the tube by a mineral oil bubbler. The flow was set to approximately 50 mL/min, and the tube was purged at this rate for at least 0.5 h before introduction of the sample. The sample to be pyrolyzed was placed in a Coors porcelain boat

(17) Sharma, R. C.; Chang, Y. A. *Bull. Alloy Phase Diagrams* **1986**, *7*, 72.

(18) (a) Natl. Bur. Stand.; PDF-2 File No. 8-487; International Centre for Diffraction Data, Newtown Square, PA. (b) Brebrick, R. F. PDF-2 File No. 25-0465; International Centre for Diffraction Data, Newtown Square, PA. (c) Scheer, M.; McCarthy, G. J.; Seidler, D.; Boudjouk, P.; PDF-2 File No. 46-1210; International Centre for Diffraction Data, Newtown Square, PA. (d) Bis R. F.; Dixon, J. R. *J. Appl. Phys.* **1969**, *40*, 1918. (e) Brebrick, R. F. *J. Phys. Chem. Solids* **1971**, *32*, 551.

Table 5. X-ray Powder Diffraction Data for SnTe.

hkl	*D*(obs), Å	*D*(calc),[a] Å	*D*,[18c] Å	2θ(obs), deg	2θ(calc),[a] deg	2θ,[18c] deg	*I*(obs),[b] %	*I*(calc),[c] %	*I*,[18c] %
200	3.1547	3.1548	3.1630	28.266	28.265	28.190	100	100	100
220	2.2308	2.2308	2.2370	40.400	40.400	40.283	78	69	52
222	1.8214	1.8214	1.8266	50.035	50.036	49.884	25	23	15
400	1.5774	1.5774	1.5819	58.461	58.461	58.278	11	11	8

[a] *D*-spacings and 2θ values calculated from the unit cell value obtained in this study using linear least-squares refinement. [b] Intensities given as peak heights for fixed divergence slit optics. [c] *I*(calc) calculated using Materials Data Inc. POWD software.

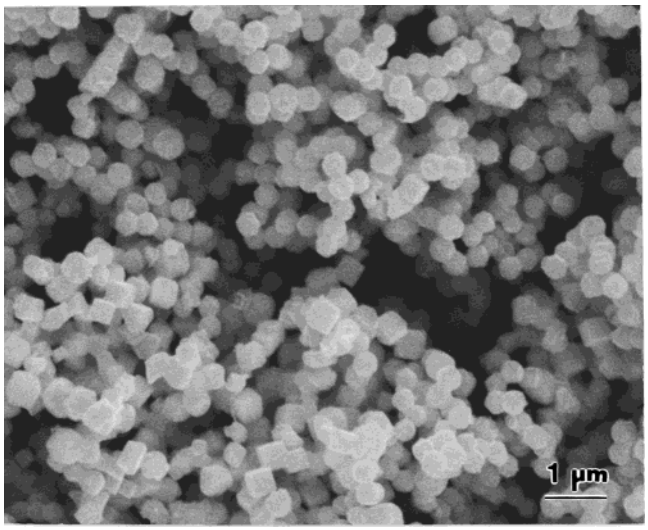

Figure 3. SEM micrograph (10 000× magnification; 15 keV) of SnTe crystals from decomposition of $(Bn_2SnTe)_3$ at 275 °C for 10 h.

that had been oven-dried at 120 °C and cooled under a stream of dry nitrogen in the tube furnace. Typical sample sizes were 500−800 mg. The crucible containing sample was placed in the tube at the center of the furnace. For all samples, the oven was programmed to ramp at a rate of 5 °C/min to 60 °C, held at this temperature for 20 min, and ramped at a rate of 5 °C/min to the final temperature. This temperature was maintained for 10 h for the reactions at 200 and 275 °C and for 5 h for the reactions at 400 °C. The products were cooled slowly to room temperature under a constant flow of nitrogen. The volatile products were condensed near the exit of the tube using dry ice and were collected by washing the tube with acetone and hexane.

Characterization. NMR spectra were obtained on a JEOL GSX270 or GSX400 spectrometer at the following frequencies: ^{1}H (270.17 MHz), ^{13}C (67.94 MHz), ^{119}Sn (149.08 MHz), ^{125}Te (126.08 MHz). Typical samples were prepared as 0.1−0.2 M solutions in $CDCl_3$. Chemical shifts are reported relative to Me_4Si for ^{1}H and ^{13}C, Me_4Sn for ^{119}Sn, and Me_2Te for ^{125}Te and are in ppm. Infrared data were recorded as KBr pellets on a Matheson Instruments 2020 Galaxy Series spectrometer and are reported in cm^{-1}. Melting points were taken on a Thomas-Hoover capillary melting point apparatus and are uncorrected. Combustion analyses were performed by Galbraith Laboratories, Knoxville, TN. Scanning electron microscopy was performed on plasma sputtered (Au) samples using a JEOL JSM6300V instrument. X-ray powder diffraction patterns were recorded from hexane slurry samples mounted on glass slides using a Philips automated vertical diffractometer with a graphite diffracted beam monochromator and variable divergence slit and using Cu Kα (λ = 1.5418 Å) radiation. NIST 660 lanthanum hexaboride (LaB_6) was used as an internal *d*-spacing standard.

Single-Crystal X-ray Diffraction Experimental Details. Details of the crystal data and a summary of data collection parameters for $(Bn_2SnTe)_3$ are given in Table 1. Data were collected on a Siemens P4 diffractometer using graphite-monochromatized Mo Kα (0.71073 Å) radiation. The check reflections, measured every 100 reflections, indicated a less than 5% decrease in intensity over the course of data collection, and hence, no correction was applied. All calculations were performed using the Siemens software package SHELXTL-Plus. The structure was solved by direct methods and successive interpretation of difference Fourier maps, followed by least-squares refinement. All non-hydrogen atoms were refined anisotropically. The hydrogen atoms were included in the refinement in calculated positions using fixed isotropic parameters.

Synthesis of $(Bn_2SnTe)_3$. Al powder (0.75 g, 28 mmol) and Te powder (1.28 g, 10 mmol) were added to a 250 mL, two-necked, round-bottomed flask containing a stirbar, N_2 inlet, a septum, and degassed distilled water (40 mL). Aqueous NH_4OH (14 mL of a 5.0 M solution, 70 mmol) was added to this mixture by syringe, forming a violet color in 10 min. The mixture was stirred for 48 h, during which time the color lightened. This mixture was transferred slowly (15 min) via cannula to an ether solution (110 mL) of Bn_2SnCl_2 (2.97 g, 8 mmol).[10c] The mixture turned dark brown and was stirred for 12 h at room temperature. Removal of the solids by filtration under nitrogen produced a filtrate that formed two layers. The organic layer was removed by cannula and the aqueous layer extracted with ether (2 × 75 mL). The organic layers were combined and evaporated to give $(Bn_2SnTe)_3$ (2.92 g, 85%) as a bright yellow solid. $(Bn_2SnTe)_3$ turns gray upon prolonged exposure to direct light or air. Recrystallization from ether provides bright yellow crystals suitable for single-crystal X-ray diffraction.

Mp: 115−116 °C (dec). ^{1}H NMR ($CDCl_3$, 270 MHz): δ 2.91 (s, 12H, PhCH_2), 6.95 (m, 12H, Ph*H*), 7.10 (m, 6H, Ph*H*), 7.21 (m, 12H, Ph*H*). ^{13}C NMR ($CDCl_3$, 67.94 MHz): δ 27.44 (Ph*C*H_2), 124.98, 127.90, 128.77, 139.55 (Ar). ^{119}Sn NMR ($CDCl_3$, 149.08 MHz): δ −148.54 [$^{1}J(^{119}Sn-^{125}Te)$ = 1615 Hz]. ^{125}Te NMR ($CDCl_3$, 126.08 MHz): δ −893.47 [$^{1}J(^{125}Te-^{119}Sn/^{117}Sn)$] = 1624/1554 Hz. IR (KBr, cm^{-1}): 3075 w, 3021 w, 1597 s, 1489 vs, 1208 w, 1045 s, 754 vs, 694 vs. Anal. for $C_{42}H_{42}Sn_3Te_3$: found (calc) C 38.94 (39.24), H 3.13 (3.29).

Acknowledgment. Financial support from the Office of Naval Research (Grant N00014-96-11271) and the National Science Foundation (Grant OSR 9452892) is gratefully acknowledged. M.R. is thankful for a North Dakota EPSCoR Doctoral Dissertation Fellowship. We also thank Kathy Iverson, Scott Payne, and Dr. Thomas Freeman for obtaining the electron micrographs and Dr. David A. Atwood for obtaining and solving the single-crystal X-ray diffraction data.

Supporting Information Available: Crystallographic tables, structure factor tables, and figures. This material is available free of charge via the Internet at http://pubs.acs.org.

OM990506U